Edited by Heinrich Hora
and George H. Miley

Laser Interaction

and Related Plasma Phenomena

Volume 6

SPACE AND TIME EVOLUTION OF SBS ION WAVES AND HARMONICS*

C. E. Clayton, C. Joshi, and F. F. Chen

Department of Electrical Engineering
University of California, Los Angeles
Los Angeles, CA 90024

INTRODUCTION

As laser fusion evolves into high intensity and long scale length experiments, stimulated Brillouin scattering [1,2] (SBS) may prove to be a large factor in the overall laser-plasma coupling efficiency. Past experiments with prepulses on solid targets showed greatly enhanced Brillouin backscatter due to the longer plasma scale lengths.[3] It may be that the severity of Brillouin backscatter is ultimately determined by the saturation level of the SBS-driven ion acoustic wave.

Until recently,[4] the only diagnostic used to study the SBS instability has been the Brillouin scattered light itself. However, the physics of the interaction is more richly revealed by studying the SBS ion wave. Here we present the results of such a study using collective ruby-laser Thomson scattering as the ion wave diagnostic. In our CO_2 laser-gas target experiment,[5] we find that the ion wave amplitude grows and saturates along with the Brillouin backscatter as incident CO_2 power in increased. The ion wave saturates at an amplitude $8\% < \tilde{n}/n_o < 20\%$. The interaction length L (the length over which the ion wave is excited) is measured to be greater than 6 mm or $L/\lambda_o > 600$ where λ_o is the wavelength of the CO_2 laser. The ion wave is found to vary exponentially in amplitude along L in agreement with convective SBS theory. The ω- and k-spectrum of the ion wave is measured and we find a large second and third harmonic content. The observed spectrum is consistent with the Fourier spectrum of a steepened wave.

*Work supported by: NSF ECS 80-03558 and DOE DE-AS08-81DP40135, 40163.

EXPERIMENTAL APPARATUS

The experimental arrangement is shown schematically in Fig. 1. The CO_2 laser delivers around 40 J in a 40 ns FWHM pulse, the peak power of which is about 400 MW. The CO_2 beam is focused with an f/7.5 lens to a vacuum intensity of about 5×10^{11} W/cm^2. The target is 8T of partially ionized nitrogen gas. The preionization is accomplished with an arc discharge. Brillouin backscattered light is collected by the input lens and split off for diagnostics. The ruby probe beam comes in at nearly a right angle to the CO_2 beam. Thomson scattered ruby light is collected with f/10 optics and imaged onto a photomultiplier, a streak camera, or a spectrograph/optical multichannel analyzer combination. The plasma density is diagnosed with ruby interferometry and is found to be around 2×10^{17} cm^{-3} or 2% of the CO_2 laser critical density.

THEORY

SBS Theory

The theory which best describes Brillouin backscatter for our experimental conditions is the theory of convective Brillouin scattering off heavily damped ion waves over a finite interaction length.[6] We have previously found quantitative agreement between this theory and experiment.[5] The theory predicts that the Brillouin scattered wave field grows exponentially from a noise level A_n at

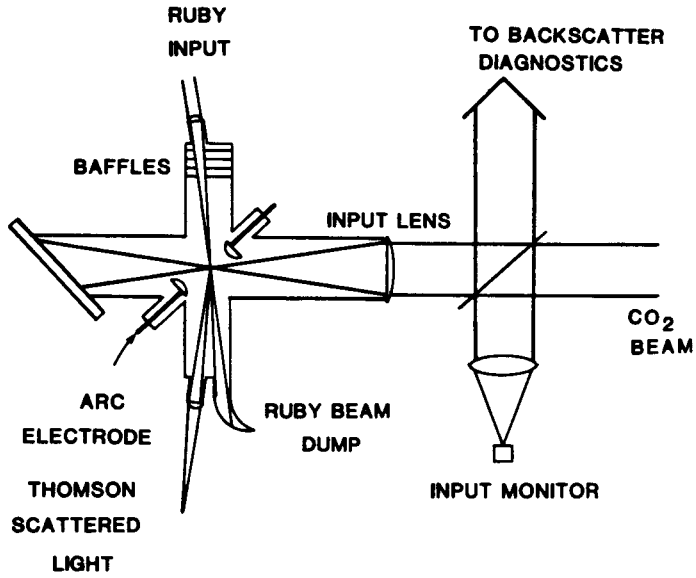

Fig. 1. Experimental setup for SBS and Thomson scattering measurements.

$z = 0$ to a level $A_s(z)$ given by

$$A_s(z) = A_n \exp (K_g z) \qquad (1)$$

where z increases towards the input end of the interaction length and K_g is the inverse gain or e-folding length given by

$$K_g = \frac{4\pi r_o}{mc^2 \omega_o} \frac{\omega_{pi}^2}{\omega_{ac}\gamma_{ac}} I_o. \qquad (2)$$

Here, $r_o = e^2/mc^2$ is the classical electron radius, ω_o is the (CO_2) pump frequency, ω_{pi} is the ion plasma frequency, $\omega_{ac}(\gamma_{ac})$ is the ion acoustic wave frequency (damping rate) and I_o is the pump intensity. We have neglected pump depletion in the above derivation. In an experiment, the input intensity has a radial dependence (transverse to z) and so the scattered wave sees a radial gain profile. If the pump spot size is much greater than the pump wavelength, then significant narrowing of the backscattered beam can occur as it is amplified along z. As a result of this "gain narrowing" of the scattered beam, the scattered power at $z = L$, given by

$$P_s(L) = P_n e^N f(N), \qquad (3)$$

where $N \equiv 2K_gL$, is reduced over the 1-D calculation by the factor $f(N)$ which is approximately $1/N$ for $N > 1$ and approaches unity as N goes to zero.

Experimentally, we are interested in the behavior of the ion wave. In our theoretical model, the ion wave amplitude is proportional to the scattered wave amplitude and so it, too, grows exponentially with z and with pump intensity. The ion wave can also exhibit the "gain narrowing" effect, that is, it can vary in diameter along z. The peak value of the ion wave is at $z = L$ and is

$$\tilde{n}/n_o(\max) \simeq \frac{N^{3/2}}{2} \left(\frac{2}{\pi} \frac{n_c}{n_o} \frac{\lambda_o}{L} \right) \sqrt{R} \qquad (4)$$

where $R = P_s(L)/P_o$ is the Brillouin reflectivity, n_o is the background electron density, n_c is the critical density for the pump radiation of wavelength λ_o, and we have used the approximation $f(N) \simeq 1/N$.

Thomson Scattering Theory

The theory for Thomson scattering of a probe laser beam from a single, large amplitude ion acoustic wave is analogous to Bragg scattering[7] of X-rays from the periodic electron distributions in crystals. The discrete planes of electrons in crystals are replaced

by sinusoidially varying electron bunches, the phasing of the bunches traveling at the acoustic velocity. As in Bragg scattering, the radiation field of each electron oscillating in the probe beam's electric field is calculated and the total field is found by intregrating over all the electrons in the scattering volume. We find that the scattered intensity is maximized if $\Delta\underline{k} \equiv \underline{k}_i - \underline{k}_s = \pm\underline{k}_{ac}$ is satisfied, where $\underline{k}_i$ and $\underline{k}_s$ are the wave vectors of the incident probe wave and scattered probe wave, respectively, and $\underline{k}_{ac}$ is that of the ion acoustic wave. For SBS backscatter, $\underline{k}_{ac} \simeq 2\underline{k}_o$. The scattered light is also frequency shifted to the red or blue by $\Delta\omega \equiv \omega_i - \omega_s = \pm\omega_{ac}$. Since $\omega_{ac} << \omega_i$, we have $k_s \simeq k_i$ so that the scattering geometry must satisfy the Bragg condition

$$\sin(\theta_s/2) = n\lambda_i/\lambda_o \qquad (5)$$

where θ_s is the scattering angle, $\lambda_j = 2\pi/k_j$, and we have included the possibility of there being the nth harmonic of the SBS-driven (n = 1) ion wave.

It should be noted, however, that while one can do Bragg scattering in second or third order, there is no second or third order Thomson scattering unless the ion wave itself has harmonic content.

The scattered light will have a small angular spread about θ_s, and if all this light is collected, the Thomson scattered power P_{TS} is given by

$$P_{TS} = P_i \left(\frac{\pi}{2} \frac{\tilde{n}}{n_o} \frac{n_o}{n_{ci}} \frac{d}{\lambda_i} \right)^2 \qquad (6)$$

where P_i is the power in the probe beam intercepted by the ion wave, d is the thickness of the ion wave along the probe beam direction and n_{ci} is the critical density for the probe beam.

Aside from these scattering effects, there are refractive effects on the propagation of the probe beam through the ion acoustic wave.[8] Most notably, the ion wave can look like a phase grating and so the probe beam can break up into many diffracted orders. However, for $\theta_s > 2\lambda_{ac}/d$, the refractive effects average out and Thomson scattering dominates.

EXPERIMENTAL RESULTS

SBS Results

The variation in the Brillouin reflectivity with incident CO_2 power is shown in Fig. 2(a). Each point represents a single shot.

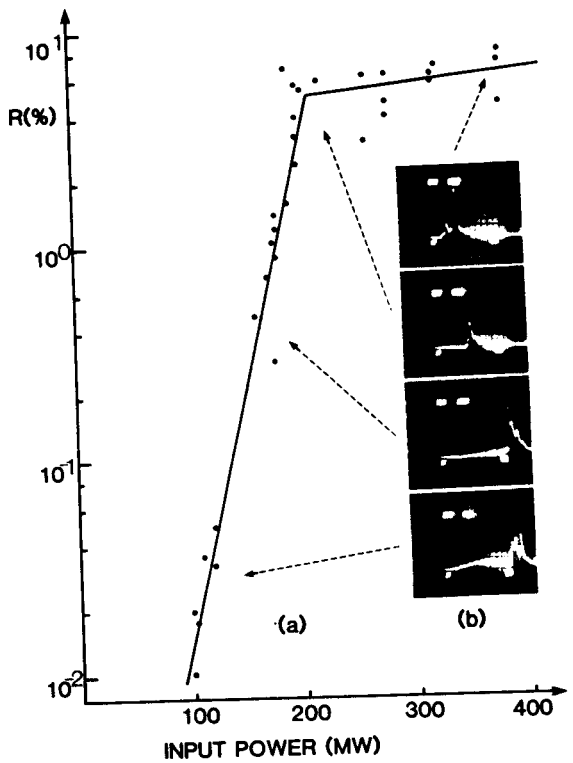

Fig. 2(a). SBS reflectivity vs. CO_2 input power. Fig. 2(b) SBS pulse shapes (10 ns/div) at various reflectivity levels.

The reflectivity grows rapidly and saturates at about 5%. The rapid growth is explained fairly well by the convective SBS theory. It is the very sudden saturation of the reflectivity which is most interesting. From Eq. (2) we see that a sudden increase in the ion wave damping rate could explain this saturation. Figure 2(b) shows typical pulse shapes of the Brillouin backscatter at various reflectivity levels. The scattering occurs in a 20 ns interval immediately following the peak of the CO_2 input pulse. However, within this interval, the SBS occurs in random 1-3 ns spikes. There is no qualitative difference in the pulse shapes above or below saturation. The peak scattered power is fairly reproducible shot-to-shot and that is what is plotted in Fig. 2(a).

To get an idea of the maximum amplitude of the ion wave at the onset of saturation, we can use Eq. (4) taking N as the number of e-foldings from the apparent noise level of Fig. 2(a) (N≈11), R = 5%, n_o/n_c = 2%, and L/λ_o = 600. This gives $\tilde{n}/n_o(max) \simeq 20\%$ so that even though the reflectivity is low, the ion wave may be large enough that nonlinearities can be turning on and saturating the ion wave.

Finally, the Brillouin backscattered light is measured to be red-shifted from the pump frequency by about 8 GHz. This implies that $ZT_e + 3T_i \simeq 260$ eV. Taking Z = 3, we have $T_e + T_i \simeq 87$ eV.

Thomson Scattering Results

The experimental arrangement in Fig. 1 shows the ruby beam focused to a point overlapping the CO_2 focus. With this arrangement we send the Thomson scattered light to a spectrograph/OMA combination and find the scattered light is blue-shifted from the ruby laser frequency by about 8 GHz. When we rotate the scattering geometry, interchanging the incident and scattering directions, the light is red-shifted by the same amount. This frequency shift is the same as that observed in the Brillouin scattered CO_2 laser light. We

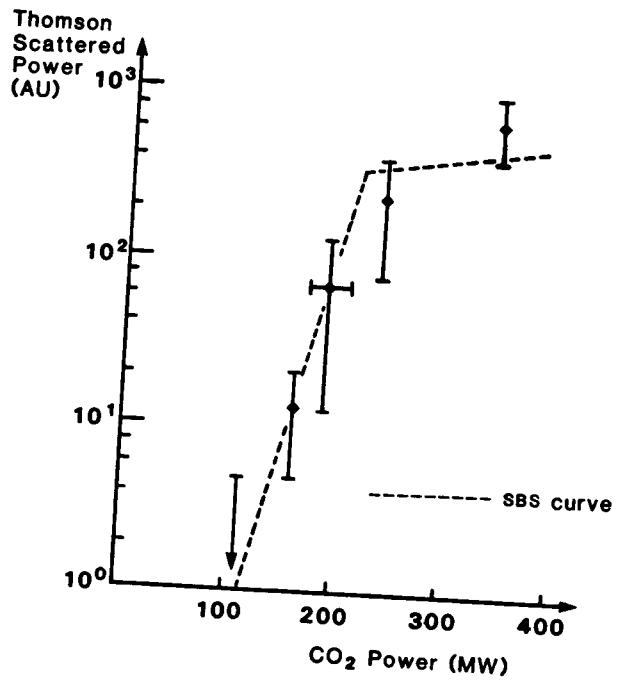

Fig. 3. Thomson scattered power ($\propto(\tilde{n}/n_o)^2$) vs. CO_2 input power. Dashed curve is SBS reflectivity.

also find that the scattered light has an angular spread (about the k-matching angle of $7\frac{1}{2}^{o}$) of only about $\frac{1}{4}^{o}$. Finally, as shown in Fig. 3, the Thomson scattered power, and thus $(\tilde{n}/n_o)^2$, grows exponentially and saturates with increasing CO_2 laser power in much the same way as does the SBS reflectivity. From these observations, it is clear that we are indeed scattering from the SBS driven ion acoustic wave.

As mentioned earlier, we have found quantitative agreement between the convective theory of SBS and our experimental observations of SBS. However, to get this agreement, we assumed that the interaction length, i.e., the length over which the ion wave is excited, was equal to the 1 cm CO_2 depth of focus. According to theory, the ion wave is not uniform over the interaction length but varies exponentially from the noise level at the downstream end to a maximum level at the CO_2 input end.

To check these predictions, we use the optical arrangement shown in Fig. 4. The cylindrical lens focuses the ruby beam to an approximately 8 mm long line focus overlapping CO_2 focal volume. Scattered light is collected at the k-matching angle of $7\frac{1}{2}^{o}$ and imaged with unity magnification onto the slit of a streak camera. Spatial variations in the ion wave amplitude show up as variations in scattered power across the slit. This 1-D image of the ion wave is streaked in time resulting in data such as shown in Fig. 5. We see that the ion wave occurs in bursts in time as does the Brillouin backscattered light. In space, the ion wave grows exponentially back towards the input end of the interaction region and then abruptly falls. This spatial behaviour is in agreement with the convective SBS theory.

We can also measure this spatial variation on a shot-to-shot basis by again focusing the ruby to point and scanning across the interaction length. This given us orders of magnitude more detection sensitivity. In this way we find that the ion wave is excited over at least 6 mm and peaks, on the average, about 2 mm to the input side of the CO_2 best focus. Thus, the interaction length is more than 6 mm or $L/\lambda_o > 600$. From interferometry, we find that the CO_2 laser produced plasma is created preferentially on the downstream end of the CO_2 depth of focus so the interaction length on the input end may be limited by plasma temperature or density gradients.

Referring again to Fig. 5, we see the axial profile of the ion wave amplitude (squared) which is responsible for reflecting 5% of the peak CO_2 laser power. This profile is equivalent to a uniform ion wave with the same peak amplitude spread over about 1 mm. In other words, the effective length of the ion wave is only about 1 mm. Therefore, a 5% CO_2 reflectivity requires a peak ion wave amplitude of about 8%. This Bragg scattering calculation does not

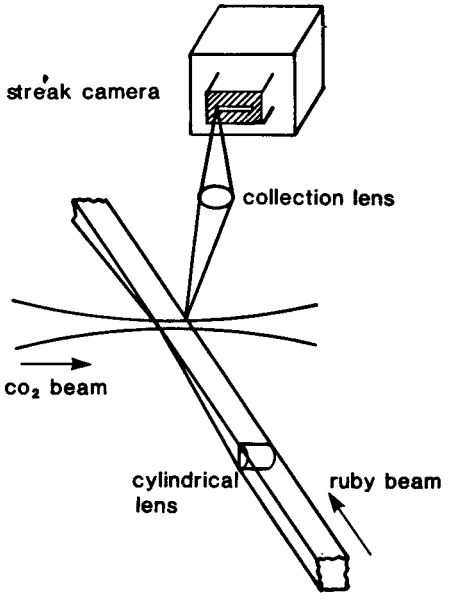

Fig. 4. Experimental arrangement used to produce streaked image data.

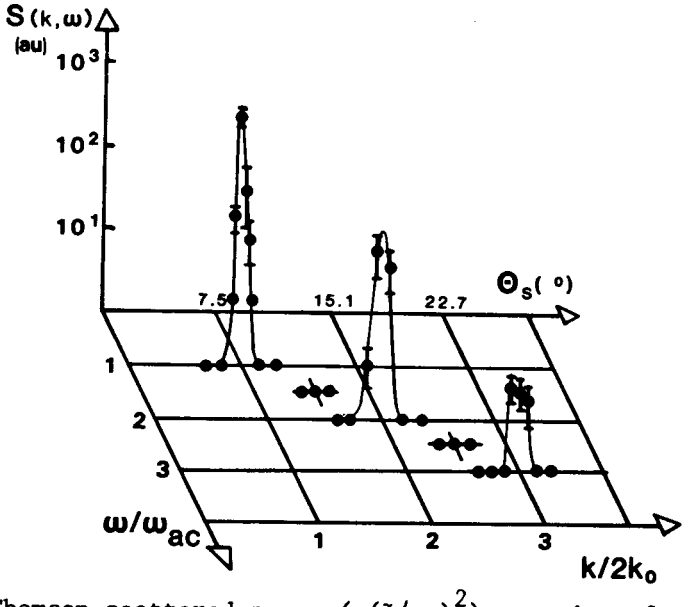

Fig. 5. Thomson scattered power ($\propto(\tilde{n}/n_o)^2$) vs. time after peak CO_2 and position along CO_2 axis. The arrow shows incident CO_2 direction.

include the possible 2-D gain narrowing effect discussed earlier. With this consideration, the ion wave amplitude could be as large as 20%.

We saw in Figs. 3 and 4 that the instability is saturated above a CO_2 input power of about 200 MW. From Eq. (2), we see that a sudden increase in the ion wave damping rate (γ_{ac}) could account for the observed saturation. One such "saturation mechanism" is harmonic generation which is predicted[9] to occur for ion wave amplitudes $\gtrsim (k_{ac}\lambda_{De})^2$ where λ_{De} is the Debye length. For smaller amplitudes, the ion wave is damped as usual by Landau and collisional damping. For larger amplitudes however, nonlinear effects cause the wave crests to steepen resulting in higher Fourier components in the k-spectrum of the wave. Since wave energy is being channeled into the harmonics, the damping rate of the fundamental is enhanced.

To see whether harmonic generation is causing our observed saturation, we measure the k-spectrum of the ion wave. This requires that we vary the scattering angle according to Eq. (5). The results of five separate experiments at five different scattering angles are plotted together in Fig. 6. Here we plot the spectral density function $S(k,\omega)$ which is proportional to scattered power or $(\tilde{n}/n_o)^2$ verses ω/ω_{ac} and $k/2k_o$. We find that there are indeed harmonics in the SBS-driven ion wave as evidenced by the (measured) multiple acoustic shifts and multiple acoustic wavenumbers. No evidence of half-harmonics is found.

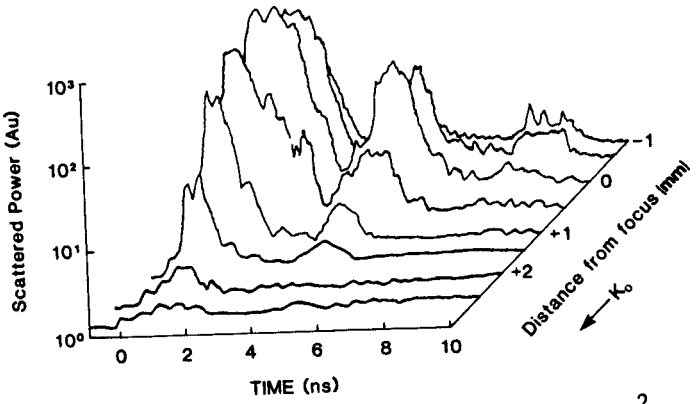

Fig. 6. Spectral density function $S(k,\omega)$ $(\propto(\tilde{n}/n_o)^2)$ vs. ω and k (or θ_s).

The angular width of the scattered light is determined by the larger of : (1) diffraction of the scattered light from the "aperature" of the ion wave, or (2) actual spectral width of the ion wave. We see that the width increases towards high harmonics implying that either the high harmonics have a broader spectrum or that the harmonics become more and more concentrated around the CO_2 laser axis.

Because the data was taken over several different experiments, there is some uncertainty as to the relative amplitudes of the various harmonics. We find that as we go to the next higher harmonic, the scattered power drops a nominal order of magnitude. This means that $\tilde{n}/n_o$ of each harmonic drops only by a factor of a few.

If the harmonics are responsible for the sudden saturation of the SBS instability; then they should suddenly appear as the CO_2 power is increased through 200 MW. They should also be strongly peaked in space, appearing only where the fundamental is largest. This, however, is not the case. The second harmonic appears throughout the ~6 mm interaction region with a similar spatial variaion to that of the fundamental. Also, the second harmonic persists even at low CO_2 power. For these reasons, we cannot attribute the observed saturation soley to harmonic generation.

As mentioned before, harmonic generation due to wave steepening is predicted to occur when the fundamental has an amplitude $\tilde{n}/n_o \sim (k_{ac}\lambda_{De})^2$ which is about 1.5% for our conditions. In our experiment, the second harmonic is first observed when the power scattered from the second harmonic rises above detection threshold. This occurs when the amplitude of the fundamental is around 1%. Therefore, the presence of harmonics is not inconsistent with the above threshold. Moreover, if we plot the sum A of the three experimentally implied sinusoids, namely

$$A = 10 \sin(k_{ac}z) + 3.3 \sin(2k_{ac}z) + \sin(3k_{ac}z), \qquad (7)$$

versus $k_{ac}z$, we get a waveform which is steepened suggesting that the observed harmonics may well be the Fourier components of a steepened ion acoustic wave. If this is true, then wave steepening occurs near the lowest measured ion wave amplitude ($\lesssim$ 1%) and little further steepening occurs as we drive the wave to larger amplitudes.

Conclusions

We have found that the Thomson scattered light at $7\frac{1}{2}^o$ is frequency shifted, obeys the k-matching condition and has a dependence on CO_2 power similar to the Brillouin scattered light. Thus we are clearly scattering from the ion acoustic wave driven by the SBS instability.

The streaked image of the ion wave shows, for the first time, that the spatial variation of the ion wave is consistent with the prediction from the convective SBS theory. We find that ion wave peaks at the input end of the ≳6 mm interaction length.

We infer the maximum or saturated level of the ion wave to be around $8\% \geq \tilde{n}/n_o \leq 20\%$. Although the interacion length and the maximum ion wave amplitude are both quite large, the SBS reflectivity is low due to the small effective length of the ion wave.

The ion wave is found to contain discrete second and third harmonics. The dependence of the amplitude of the second harmonic on CO_2 laser power as well as its spatial variation imply that harmonic generation is not responsible for the observed saturation of the SBS instability. The appearance of harmonics in an ion wave of amplitude > 1% is not inconsistent with the theory of harmonic generation due to wave steepening. In fact, our observed ion acoustic wave spectrum is consistent with the Fourier spectrum of a steepened wave.

References

1. J. F. Drake, P. K. Kaw, Y. C. Lee, G. Schmidt, C. S. Liu, and M. N. Rosenbluth, Parametric instabilities of electromagnetic waves in plasmas, Phys. Fluids 17:778 (1974).
2. D. W. Forslund, J. M. Kindel, and E. L. Lindman, Theory of stimulated scattering processes in laser-irradiated plasmas, Phys. Fluids 18:1002 (1975).
3. B. H. Ripen, F. C. Young, J. A. Stamper, C. M. Armstrong, R. Decoste, E. A. McLean, and S. E. Bodner, Enhanced backscatter with a structured laser pulse, Phys. Rev. Lett. 39:611 (1977).
4. C. E. Clayton, C. Joshi, and F. F. Chen, Thomson scattering from ion acoustic waves associated with stimulated Brillouin scattering, Bull. Amer. Phys. Soc. 26:933 (1981).
5. C. E. Clayton, C. Joshi, A. Yasuda, and F. F. Chen, Dependence of stimulated Brillouin scattering on target material and f number, Phys. Fluids 24:2312 (1981).
6. W. L. Kruer, Nonlinear estimates of Brillouin scatter in plasmas, Phys. Fluids 23:1273 (1980).
7. L. D. Landau and E. M. Lifshitz, "Electrodynamics of Continous Media", Pergamon Press, New York (1960).
8. W. R. Klein and B. D. Cook, Unified approach to ultrasonic light diffraction, IEEE Trans. Sonics and Ultrasonics SU-14:123 (1967).
9. J. M. Dawson, W. L. Kruer, and B. Rosen, Investigation of ion waves, in "Dynamics of Ionized Gases", M. Lighthill, I. Imai, and H. Sato, eds., University of Tokyo Press, Tokyo (1973).